A NOVEL Z-SCHEME HETEROSTRUCTURED AgI/AgFeO$_2$ COMPOSITES AS AN EFFICIENT VISIBLE-LIGHT PHOTOCATALYST FOR THE DEGRADATION OF RHODAMINE B

Z. SONG[*], Y.Q. HE, F. WANG

College of Chemistry, Changchun Normal University, Changchun 130032, Jilin, People's Republic of China

This paper reported a novel Z-scheme heterostructured AgI/AgFeO$_2$ composite was synthesized by a facile precipitation method and its physicochemical property was characterized by XRD, SEM, EDS etc. The AgI particles were successfully loaded on the surface of the AgFeO$_2$ particles. The photocatalytic performances of AgI/AgFeO$_2$ composites were studied using Rhodamine B (RhB). As compared to pure AgFeO$_2$, the Z-scheme heterostructured AgI/AgFeO$_2$ photocatalysts exhibited superior degradation and stability in the visible-light region. The removal of RhB solution via I/Fe-3 composite was about 98.31% within 60 min. For the enhanced photocatalytic property of the AgI/AgFeO$_2$ composites, the effective electron-hole separation and close interphase contact coupling of AgI and AgFeO$_2$ may play important roles. The cyclic characterization and active specials trapping experiments indicated that the structure of Z-scheme can obviously enhanced the efficiency of photogenerated electron-hole pairs and produce more •O$_2^-$, which played a dominant role in the removal of dye of RhB.

1. Introduction

For solving environmental pollution, novel functional materials have attracted tremendous attention for treatment of organic dye due to their great potential properties [1-6]. Silver halide (AgX, X: Cl, Br, I) is well-known as a photosensitive material, and has been widely applied in photographic field [7-9]. Under visible light irradiation, silver halide nanostructures can promote electron transfer and restrain electron-hole recombination. Especially, in the visible-light spectrum, band gaps of AgI nanostructures are suitable for photocatalysis [10-11]. However, due to unstable property of AgI, it is easy to decompose into Ag^0 under light irradiation, thereby limiting the practical photocatalytic application. AgI was dispersed upon support materials to form a heterojunction structure, and shown to have increased stability and photocatalytic activity [12].

Recently, Ag-based multimetal compounds have been intensely studied because of their promising photocatalytic property [13]. Under visible light irradiation, AgMO$_2$ (M = Sc, Cr, Fe, Co, Ni, Rh) are the useful contenders due to their strong catalytic property and high adsorption capacity [14-16]. Among all kinds of above components, AgFeO$_2$ was found to easily absorb visible light to yield photogenerated electrons and holes due to its narrow band gap energy. Thus, AgFeO$_2$ is considered to have the potential property for photocatalytic application under visible light irradiation. To the best of our knowledge, there have no works been reported to the fabrication of AgFeO$_2$ with AgI in the synthesis, visible light activity and photocatalytic mechanism.

Herein we report a newly constructed AgI/AgFeO$_2$ composite with different content of AgI

---

[*]Corresponding author: songzheszh@126.com

by adjusting the mass of AgNO$_3$ and NaI, and AgI/AgFeO$_2$ composite is expected to exhibit high photocatalytic activity under visible light irradiation.

2. Experimental

2.1. Materials

AgNO$_3$, Fe(NO$_3$)$_3$·9H$_2$O, NaOH, NaI and other reagents were obtained from commercial sources. All the chemicals used in this work without further purification.

2.2. Preparation of AgFeO$_2$ composite

Pure AgFeO$_2$ was synthesized via a hydrothermal method as follows: AgNO$_3$ (0.85g) and Fe(NO$_3$)$_3$·9H$_2$O (2.02g) were dissolved into 75 mL of deionized water to obtain solution A. NaOH (1.50g) was added into the mixture A as precipitating agent under magnetic stirring for 30 min, thus forming suspension mixture B. Then the suspension mixture B was transferred into 100 ml Teflon-lined stainless steel reactor and heated to 180°C for 24 h under autogenous pressure. The mixture was allowed to cool to room temperature and the as-prepared precipitate was filtered, washed three times with deionized water and dried in an oven at 60°C for 12 h.

2.3. Preparation of different proportion of AgI/AgFeO$_2$ sample

Preparation of AgI/AgFeO$_2$ (mole ratio is 3:1 of AgI to AgFeO$_2$) sample: AgFeO$_2$ (0.392g) and AgNO$_3$ (1.020g) were dispersed in 30 mL of deionized water by ultrasonication, thus forming suspension mixture A. NaI (6.180g) was added in 10 ml deionized water formed solution B, and the solution B was added dropwise in mixture A under vigorously stirring for 20 min. The resulting precipitates were collected and washed with deionized water and dried at 60°C for 12 h. The AgI/AgFeO$_2$ (3:1) sample was marked as I/Fe-3. Different AgI/AgFeO$_2$ samples were obtained by adjusting the mole ratio of AgNO$_3$ and NaI, and the as-synthesized AgI/AgFeO$_2$ photocatalysts were marked as I/Fe-0.5, I/Fe-1, I/Fe-2, I/Fe-3 and I/Fe-4, respectively. (I means AgI, Fe means AgFeO$_2$).

2.4. Characterization of catalytic

The crystalline structure of composites was characterized by X-ray diffraction (2θ ranged from 10° to 80°). The morphological features of the composites were characterized by using a scanning electron microscope (SEM). The surface composition of the composites was ascertained by using the Energy Dispersive Spectroscopy (EDS), which connected with SEM.

2.5. Photocatalytic experiments

The photocatalytic activity of the samples was evaluated by degradation of RhB solution under the radiation of a 300 W Xe lamp. Typically, 0.05 g of the sample was added into 100 ml of RhB solution (10 mg/L) in dark for 40 min to achieve absorption equilibrium between dye and photocatalyst. Then about 3mL of suspension was withdrawn and collected by centrifuging at 5000 rpm for 10 min. The top clear solution of RhB was analyzed by a UV-vis spectrophotometer (UV-1600) at wavelength of 554 nm.

3. Results and discussion

3.1. Characterization

The phase and crystal structures of the obtained samples were carried out by XRD analysis. Fig. 1 shows the XRD patterns for AgI, AgFeO$_2$ and AgI/AgFeO$_2$. As shown in Fig. 1, the peaks of the XRD pattern for AgI can be indexed to pure AgI (JCPDS, No. 09-0399). All the diffraction peaks of AgI at 23.71°, 39.13°, 46.31°, 56.67°, 62.26°, 71.03°, 76.08° can be indexed to crystallite planes of (111), (220), (311), (400), (331), (422), (511). As for the AgFeO$_2$ (JCPDS, No. 21-1081),

the strong diffraction peaks at 14.27º, 28.77º, 34.41º, 35.42º, 39.32º, 43.78º, 52.48º, 60.98º, 68.82º, 72.54º can be indexed into crastallite planes of (003), (006), (101), (102), (104), (009), (108), (110), (116), (202). Over $AgI/AgFeO_2$ composites, characteristic peak of AgI and $AgFeO_2$ are observed, and no other peaks of any impurities are observed.
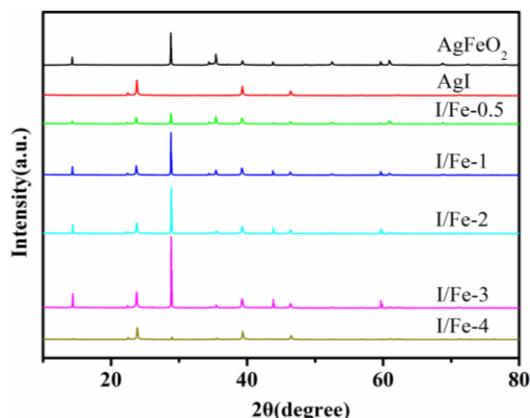
Fig. 1. XRD patterns of pure $AgFeO_2$, pure AgI and $AgI/AgFeO_2$ composites
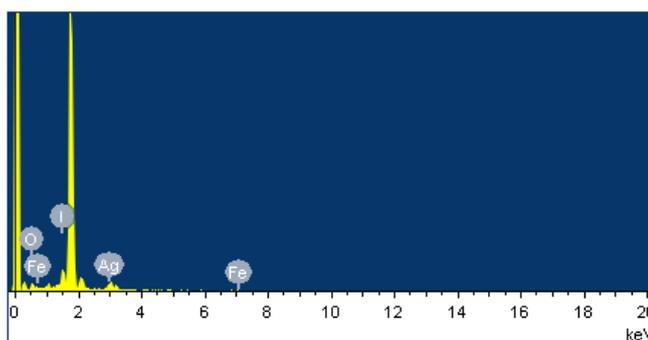
Fig. 2. The EDS patterns of I/Fe-3 composite

As can be seen in Fig. 1, in terms of I/Fe-3 composite, the intensities of diffraction peaks were the strongest. In addition, combined with photocatalytic experiment results, the chemical composition of as-prepared I/Fe-3 composite can obviously increase the catalytically active sites. The chemical composition of as-prepared I/Fe-3 composite was recorded by the EDS spectrum which shown in Fig. 2. It can be found that only elements Ag, I, Fe, Si, and the signals of Si resulting from silicon slice, indicating that the composites of $AgI/AgFeO_2$ were obtained.

3.2. Morphology analysis

The shape and size of the pure $AgFeO_2$, AgI and I/Fe-3 was examined by SEM. The as-synthesized pure $AgFeO_2$ (Fig. 3(a)), mainly contains layer structure and have a mean diameter of 500 nm. As can be seen in Fig. 3(b), pure AgI composed of spherical-like particles with size of about 1-2 μm. Comparing the morphology of $AgI/AgFeO_2$ hybrids, it clearly suggests that spherical-like particles AgI inlay with the layer $AgFeO_2$ to obtain a heterojunction structure composite (Fig. 3(c), and the possible growth process of I/Fe-3 was shown in Scheme 1.) The tight structure between AgI and $AgFeO_2$ would promote the electron-hole separation and expedite the transfer of photogenerated carriers.
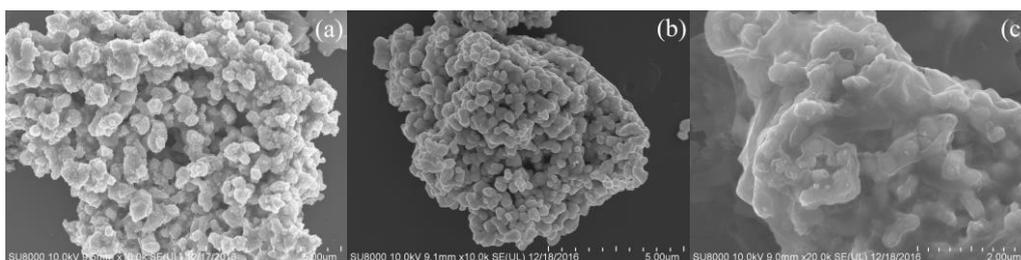
Fig. 3 SEM imagines of (a) AgFeO₂, (b) AgI and (c) I/Fe-3
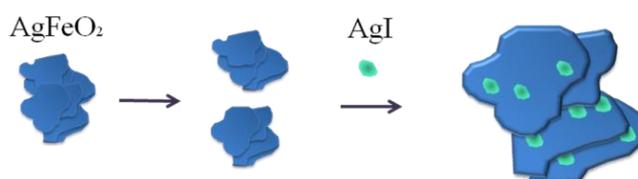
Scheme 1. Schematic representation of the growth mechanism of I/Fe-3 heterostructures

3.3. Photocatalytic activity of photocatalyst

The photocatalytic activities of as-prepared samples for the degradation of the Rhodamine (RhB) dye (10 mg/L, pH=4.8) were evaluated under visible light irradiation at room temperature for 60 min. As shown in Fig. 4, pure $AgFeO_2$ exhibits low photocatalytic performance for RhB degradation. Noteworthy, as compared to the pure $AgFeO_2$, the heterojunction composites with different molar ratio of AgI to $AgFeO_2$ presented prominently enhanced photocatalytic activity under simulated solar light irradiation for 60 min, and the most excellent photocatalytic performance was the I/Fe-3. This might indicate that close interphase contact coupling of AgI and $AgFeO_2$ nanoparticles in $AgI/AgFeO_2$ hybrids should play a dominant role in enhancing the photoreactivity.

Besides, the reusability and stability of I/Fe-3 photocatalyst was evaluated via a cycle experiment. The results were shown in Fig. 5, after three-recycled test, the I/Fe-3 photocatalyst exhibited a stable photocatalytic performance. This suggested that I/Fe-3 possessed good chemical stability in the usage process.
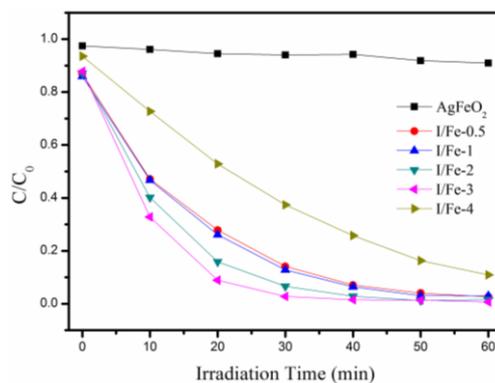
Fig.4 Photocatalytic degradation of RhB with different as-prepared photocatalyst
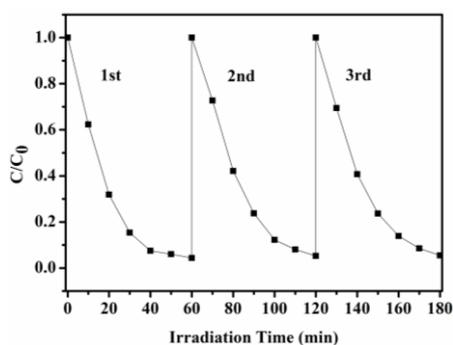
Fig. 5. Cycling runs for degradation of RhB by I/Fe-3

3.4. Active species analysis

For the purpose of further detection the active species, isopropano (IPA), benzoquinone (BQ) and $(NH_4)_2C_2O_4$ (AO) were introduced into photocatalytic degradation system, respectively. As depicted in Fig. 6, when IPA or AO was added into the system, the degradation efficiency of RhB via I/Fe-3 hardly reduced. However, by using BQ as scavenger, the photocatalytic efficiency decreased obviously.
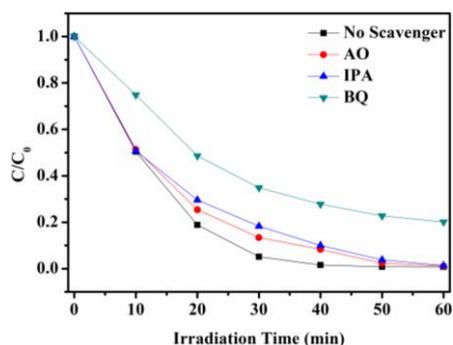
Fig.6. Results of active species detection during the photocatalytic degradation of RhB via I/Fe-3

It may mainly ascribe to that the $\cdot O_2^-$ was established as the main reactive species and it can be inferred that the photodegradation of RhB on $AgI/AgFeO_2$ composites is mainly attributed to $\cdot O_2^-$.

3.5. Reaction mechanism

On the basis of the above experiments and discussions, a possible photocatalytic mechanism of I/Fe-3 catalyst was proposed as illustrated in Scheme 2. As shown in the scheme 2, the VB is the valence band, and the CB is the conductive band. The VB and CB edge of $AgFeO_2$ were 1.81 eV vs. NHE and 0.51 eV vs. NHE, respectively [17]. For AgI, the VB and CB edge were 2.38 eV vs. NHE and -0.42 eV vs. NHE [18], respectively. Forming Z-scheme heterostruction between AgI and $AgFeO_2$ might express the possible mechanism. The photo electrons were transferred from CB of $AgFeO_2$ to VB of AgI and recommendation with photo electron−hole of $AgFeO_2$. Furthermore, the CB potential of AgI (-0.42 eV) was more positive than oxygen E^0 ($O_2/ \cdot O_2^-$) = -0.046 eV vs NHE, suggesting that $\cdot O_2^-$ was produced, which played a dominant role in the

degradation of RhB. The possible electrons transfer process might be described as follows:

$$AgI + hv \rightarrow e_{CB}^- + h_{VB}^+$$

$$AgFeO_2 + hv \rightarrow e_{CB}^- + h_{VB}^+$$

$$AgI\,(e_{CB}^- + h_{VB}^+) + AgFeO_2\,(e_{CB}^- + h_{VB}^+) \rightarrow AgI\,(e_{CB}^-) + AgFeO_2\,(h_{VB}^+)$$

$$AgI\,(h_{VB}^+) + AgFeO_2\,(e_{CB}^-) \rightarrow recommendation$$

$$AgI\,(e_{CB}^-) + O_2 \rightarrow \bullet O_2^- + AgI$$

$$\bullet O_2^- + RhB \rightarrow CO_2 + H_2O$$
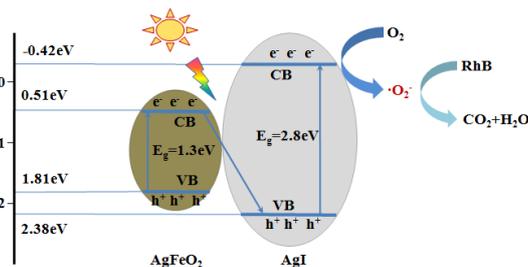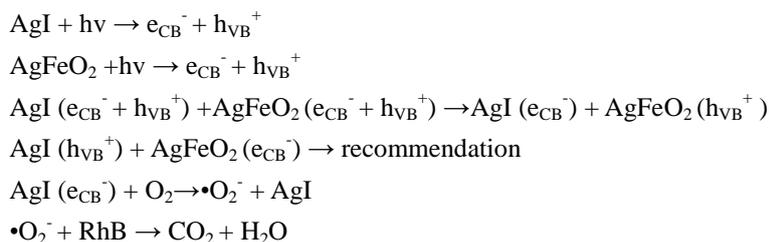
Scheme 2. The schematic possible mechanism of degradation of RhB by I/Fe-3 heterostruction

4. Conclusions

In summary, we have developed a novel Z-scheme heterostructured $AgI/AgFeO_2$ composite for dehydrogenation of RhB that exhibits high efficiency and stability under visible light irradiation. The as-obtained composites were characterized by XRD, SEM and EDS techniques. The optimized mole ratio of AgI and $AgFeO_2$ was adjusted and the I/Fe-3 composite exhibited the superior photocatalytic activity for RhB degradation. The enhanced photocatalytic property of the I/Fe-3 catalyst was found to be attributed to forming Z-scheme heterostruction between AgI and $AgFeO_2$ and the higher separation efficiency of photoinduced electrons and holes. The above properties determined the novel $AgI/AgFeO_2$ composite as a promising material for environmental application under visible light.

Acknowledgments

References

[1] D. Yue, D.M. Chen, Z.H. Wang, H. Ding, R.L. Zong, Y.F. Zhu Phys. Chem. Chem. Phys. **16**, 26314 (2014).

[2] X.N. Luan, Y. Wang Mat. Sci. Semicon. Proc. **43**, 25 (2014).

[3] Y. Q. Kou, J.K. Yang, B. Li , S. C. Fu Mater. Res. Bull. **63**, 105 (2015).

[4] J. Liu, G.K. Zhang Appl. Surf. Sci. **319**, 291 (2014).

[5] D.M. Chen, G.X. Du, Q. Zhu, F.S. Zhou J. Colloid Interface Sci. **409**, 151 (2013).

[6] X.F. Wu, L.L. Wen, K.L. Lv, K.J. Deng, D.G. Tang, H.P. Ye, D.Y. Du, S.N. Liu, M. Li, Appl. Surf. Sci. **358**, 130 (2015).

[7] X.J. Wen, C.G. Niu , M. Ruan , L Zhang , G.M. Zeng J. Colloid Interf. Sci. **497**, 368 (2017).

[8] C.S. Lei, M. Pi, X.F. Zhu, P.F. Xia, Y.Q. Guo, F.G. Zhang Chem. Phys. Lett. **664**, 167 (2016).

[9] Q. Wang, M.M. Chen, N.X. Zhu, X.D. Shi, H. Jin, Y. Zhang, Y.Q. Cong J. Colloid Interf. Sci. **448**, 407 (2015).

[10] H. F. Ye, H.L. Lin, J. Cao, S.F. Chen, Y. Chen J. Mol. Catal. A-Chem. **397**, 85 (2015).

[11] H. H. Chang , J. Lv, H.C. Zhang ,B. Zhang, W.L. Wei, Y. Qiao Biosens. Bioelectron. **87**,579 (2017).

[12] J. L. Liang, J. Deng, M. Li, M.P. Tong Colloids Surfaces B **138**, 102 (2016).

[13] S.M. Hosseinia, H. Hosseini-Monfared, V. Abbasi, M.R. Khoshroo Inorg. Chem. Commun. **67**, 72 (2016).

[14] J. Li, A.W. Sleight, C.Y. Jones, B.H. Toby J Solid State Chem. **178**, 285 (2005).

[15] A. Vasiliev, O. Volkova, I. Presniakov, A. Baranov, G. Demazeau, J.M. Broto, M. Millot, N. Leps, R. Klingeler, B. Buchner, M.B. Stone, A. Zheludev J. Phys. Condens. Matter. **22**, 1 (2010).

[16] A. Dumbrava, D. Berger, G. Prodan, F. Moscalu Dig. J. Nanomater Bios. **11**, 1189 (2016).

[17] D.D. Tang, G.K. Zhang Appl. Surf. Sci. **391**, 415 (2017).

[18] Y. Bi, S. Ouyang, J. Cao, J. Ye Phys. Chem. Chem. Phys. **13**, 10071 (2011).